Hydrogen bond Coupling in Sodium Dihydrogen Triacetate

ARTICLE *in* JOURNAL OF MOLECULAR MODELING · AUGUST 2014

Impact Factor: 1.74 · DOI: 10.1007/s00894-014-2363-9

3 AUTHORS, INCLUDING:

Rifaat Hilal

King Abdulaziz University

74 PUBLICATIONS **251** CITATIONS

SEE PROFILE

Mohamed F Shibl

Qatar University

22 PUBLICATIONS **256** CITATIONS

SEE PROFILE

J Mol Model (2014) 20:2363
DOI 10.1007/s00894-014-2363-9

ORIGINAL PAPER

Hydrogen bond coupling in sodium dihydrogen triacetate

Ashour A. Ahmed · Rifaat H. Hilal · Mohamed F. Shibl

Received: 23 April 2014 / Accepted: 22 June 2014

Abstract The coupling of hydrogen bonds is central to structures and functions of biological systems. Hydrogen bond coupling in sodium dihydrogen triacetate (SDHTA) is investigated as a model for the hydrogen bonded systems of the type O-H…O. The two-dimensional potential energy surface is derived from the full-dimensional one by selecting the relevant vibrational modes of the hydrogen bonds. The potential energy surfaces in terms of normal modes describing the anharmonic motion in the vicinity of the equilibrium geometry of SDHTA are calculated for the different species, namely, HH, HD, DH, and DD isotopomers. The ground state wave functions and their relation to the hydrogen bond structural parameters are discussed. It has been found that the hydrogen bonds in SDHTA are uncoupled, that is elongation of the deuterated hydrogen bond does not affect the non-deuterated one.

Keywords Coupling · Hydrogen bonds · Isotopomers · Potential energy surface · Wave function

Electronic supplementary material The online version of this article (doi:10.1007/s00894-014-2363-9) contains supplementary material, which is available to authorized users.

A. A. Ahmed · R. H. Hilal · M. F. Shibl
Department of Chemistry Faculty of Science, Cairo University, Giza 12613, Egypt

A. A. Ahmed
Institute of Physics, Rostock University, 18051 Rostock, Germany

R. H. Hilal
Department of Chemistry Faculty of Science, King Abdulaziz University, Jeddah, Kingdom of Saudi Arabia

M. F. Shibl
Gas Processing Center College of Engineering, Qatar University, P.O. Box 2713, Doha, Qatar

M. F. Shibl (✉)
Department of Materials Science and Engineering, Cornell University, Ithaca, NY 14853, USA
e-mail: mfshibl@cornell.edu

Introduction

Hydrogen bonds and their couplings govern molecular interactions in many biological systems. For instance, carbohydrate-protein receptor interaction in molecular recognition is controlled by hydrogen bonds of O-H… O type and their couplings. This means that the intramolecular and/or intermolecular hydrogen bonds coupling (HBC) in carbohydrates can affect their reactivity toward other molecules [1]. Replacement of one or more hydrogen atoms (of the hydrogen bond) by deuterium ones reflects the coupling in multiple hydrogen-bonded systems. Nevertheless, it is difficult to determine the hydrogen bond parameters and then the coupling in deuterated hydrogen bonds using X-ray diffraction with accuracy [2]. Although, neutron diffraction is able to measure the hydrogen bond geometric change upon deuteration, it needs expensive requirements like a neutron source, a detector, …etc. NMR method, on the other hand, can be used to detect the coupling between hydrogen bonds without the special requirements needed for the neutron diffraction [3–5]. In this respect, the information about distances obtained from hydrogen bond correlation can be correlated to NMR chemical

Published online: 20 July 2014

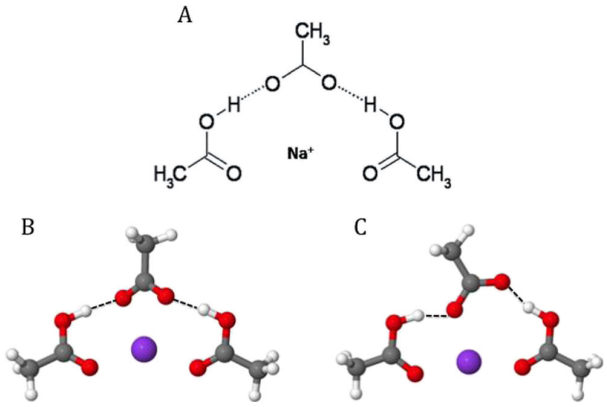

Fig. 1 The chemical structure and the lowest optimized geometries, conformers, of SDHTA at B3LYP/6-31++G(d,p) level of theory. These conformers are adapted from ref. [20]

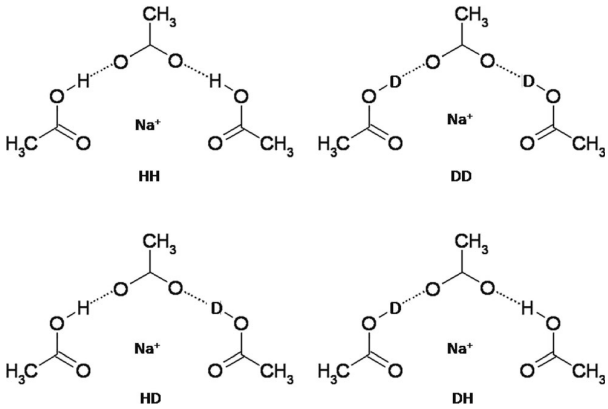

Fig. 2 The deuteration scheme for the non- (HH), double- (DD), right- (HD), and left- (DH) deuterated species

shifts of the hydrogen atoms or the heavy atoms of the hydrogen bonds [6, 7].

Theoretically HBC can be investigated by calculating, classically, the hydrogen bond parameters of multiple-hydrogen-bonded system [8]. However, this method does not include the quantum nature of hydrogen atoms. Therefore, an alternative theoretical method, based on quantum mechanical calculations including the anharmonicity in the potential energy surface, can be employed to highlight the coupling in double hydrogen bonded systems. HBC has been previously reported for simpler system like porphycene (more symmetric system with N-H…N hydrogen bond type) where coupled hydrogen bonds have been found [9, 10]. In the current contribution, the previous work is extended to cover asymmetric, more complicated, systems such as sodium dihydrogen triacetate (SDHTA) as a model mimicking the O-H-O carbohydrate intermolecular hydrogen bonds. Here, on one hand, the hydrogen bond with a hydrogen atom that bridges two similar electronegative atoms, like N-H… N or O-H…O, will be called homo-hydrogen bond. On the other hand, the mixed hydrogen bond, of the type N-H…O and/or N…H-O, will be called hetero-hydrogen bond. The purpose of such study is to establish a general and efficient method for exploring the coupling in multiple-hydrogen-bonded systems (with both homo- and hetero-hydrogen bonds). This will be of great interest to be applicable for more complicated biological molecules (with O-H…O, N-H…N, N-H…O, and N…H-O hydrogen bond types) where multiple hydrogen bonds and their cooperativity play a pivotal role [11–15].

The hydrogen diacetates of ammonium [16], sodium [17], and potassium [18] have been fully investigated, whereas there are only a few reports on the dihydrogen triacetates [19], which will be thereby investigated. In this work, single and double deuterations of SDHTA are considered. The effect of the deuteration on the anharmonicity in the potential energy surfaces that are calculated in the vicinity of the equilibrium geometry [20] for HH, HD, DH, and DD isotopomers in terms of normal mode coordinates, and then on the molecular

Table 1 The normal modes for the selected SDHTA conformer, in Fig. 1b (associated with the protons' motion), the corresponding non-scaled wave numbers (in cm^{-1}) and assignments. The molecular symmetry is C_1. DFT/B3LYP/6-31++G(d,p) level of theory was used as implemented in *Gaussian03* [24]

Sym.	ω (cm^{-1})	Int. (km mol^{-1})	Assignment
A	1025	144	Sym. combination of the O-H out-of-plane bending
A	1036	50	Asym. combination of the O-H out-of-plane bending
A	3025	2791	Asym. combination of the O-H stretching
A	3080	3080	Sym. combination of the O-H stretching

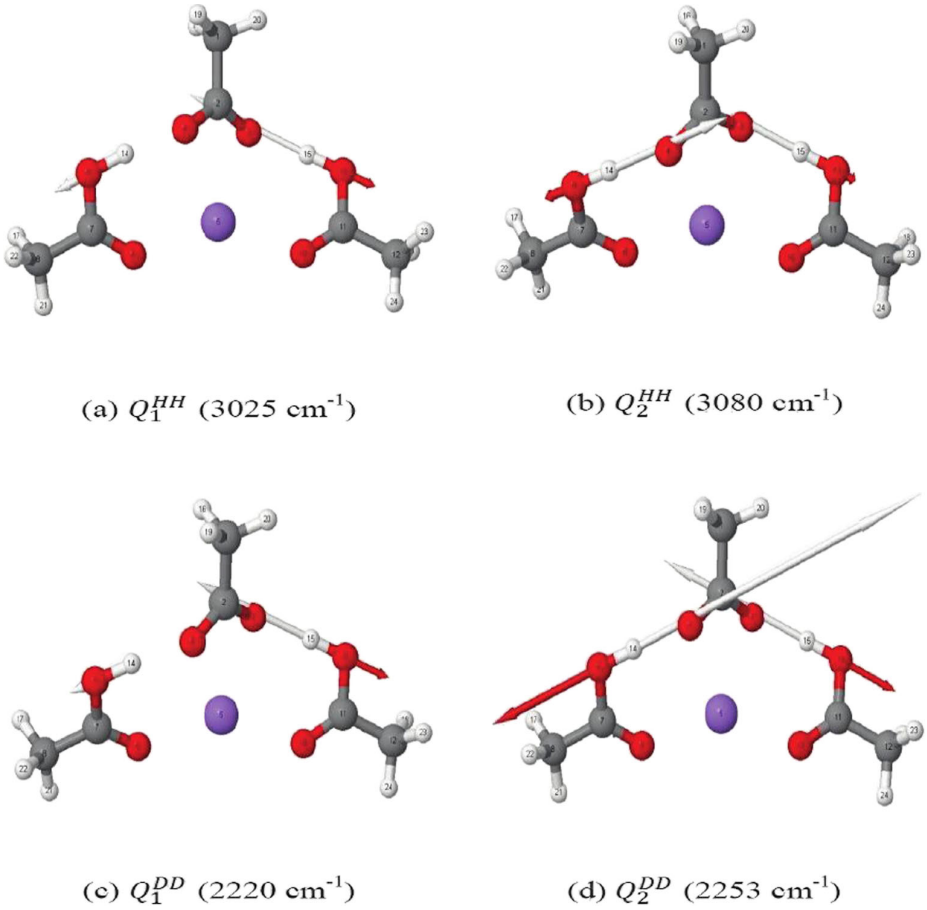

Fig. 3 The mode displacement vectors corresponding to the O-H/O-D stretching vibrations for the HH and DD species. (a) asymmetric combination of the O-H stretching; (b) symmetric combination of the O-H stretching; (c) asymmetric combination of the O-D stretching; (d) symmetric combination of the O-D stretching

wavefunctions is studied in order to probe the cooperativity in the hydrogen bonds. The structural parameters as well as the effect of deuteration on the cooperativity of the hydrogen bonds of SDHTA will be scrutinized and compared with the available NMR-experimental data.

Results and discussion

Since the three-dimensional structure of SDHTA (see Fig. 1A) was not well known, a recent study has aimed to explore the geometry and energetics of low energy conformers of SDHTA [20]. Different spatial configurations, conformers, for SDHTA have been investigated using density functional theory (DFT) at BLYP and B3LYP levels combined with different basis sets. The most stable SDHTA conformers of comparable energy, with electronic energy difference of 0.55 kcal mol^{-1}, are shown in Fig. 1. The conformer in Fig. 1B has two hydrogen bonds of higher symmetry, with respect to each other, than that for the conformer in Fig. 1C. Density functional theory based Born-Oppenheimer molecular dynamics simulations (DFT-MD) for SDHTA starting with the conformer with less symmetric hydrogen bonds, in Fig. 1C, have yielded a scenario, where both conformers are visited along the room temperature equilibrium trajectory [20]. DFT-MD gave rise to average structure closer to the one with more symmetric hydrogen bonds (Fig. 1B). Moreover, this conformer, in Fig. 1B, is in accord with the experimental findings regardless of the counter ion [21]. Therefore, the conformer, shown in Fig. 1B, will be used in the current contribution.

In order to describe a motion in the vicinity of the minimum structure, the normal mode coordinates can be employed. Some normal modes of the equilibrium geometry of SDHTA (Fig. 1B) obtained at DFT/B3LYP [22] level of theory using the 6–31++G(d,p) [23] basis set are represented in Table 1. These modes, calculated using *Gaussian03* suite of programs [24], correspond to

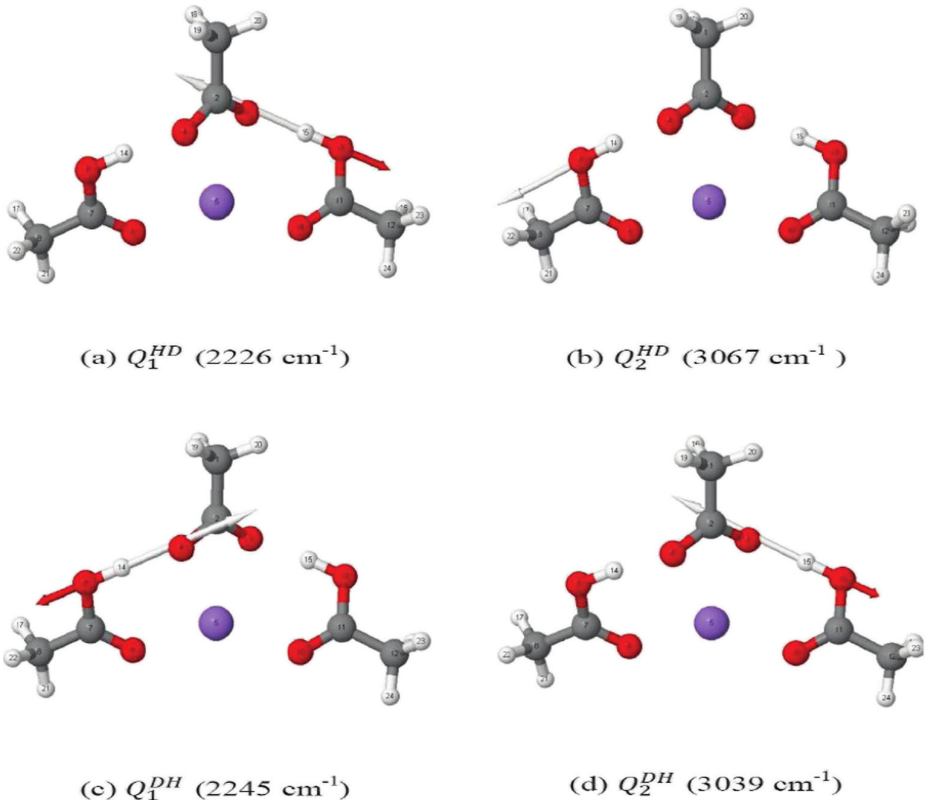

Fig. 4 The mode displacement vectors corresponding to the O-H/O-D stretching vibrations for the HD and DH species. (a) O-D stretching vibration of HD species; (b) O-H stretching vibration of HD species; (c) O-D stretching vibration of DH species; (d) O-H stretching vibration of DH species

the vibrations describing the motion of the hydrogen bond protons. Inspecting these normal modes reveals that O-H stretching modes are the most intense bands compared to the other O-H vibrations. Since the molecule is asymmetric, it should be noticed that the word symmetric or antisymmetric, mentioned in Table 1, reflects that the motion of the O-H stretching motions are in the same or opposite directions, respectively.

The Hamiltonian in Watson form (neglecting the vibration-rotation couplings) can be written in terms of the normal modes $\{Q_i\}$ and the corresponding momenta $\{P_i\}$ as [25]:

$$H = \sum_{i=1}^{3N-6} \frac{P_i^2}{2} + V(Q_1, Q_2, \ldots, Q_{3N-6}) \,, \tag{1}$$

where $V(Q_1,Q_2,\ldots,Q_{3N-6})$ is the full-dimensional potential energy surface which can be written in terms of correlated and uncorrelated contributions as [26]:

$$V(Q_1, Q_2, \ldots, Q_{3N-6}) = \sum_i V_i^{(1)}(Q_i) + \sum_{i<j} V_{ij}^{(2)}\left(Q_i, Q_j\right) + \sum_{i<j<k} V_{ijk}^{(3)}\left(Q_i, Q_j, Q_k\right) + \ldots \tag{2}$$

where the terms $V_i^{(1)}(Q_i)$, $V_{ij}^{(2)}(Q_i,Q_j)$, $V_{ijk}^{(3)}(Q_i,Q_j,Q_k)$, etc. are the uncorrelated, two-mode correlations, three-mode correlations, etc., respectively. Calculations of $V_i^{(1)}(Q_i)$ and $V_{ij}^{(2)}(Q_i,Q_j)$ are possible for systems as big as SDHTA. Nevertheless, $V_{ijk}^{(3)}(Q_i,Q_j,Q_j)$ or higher order couplings are computationally expensive for such a large system. Therefore, one may employ some approximation to make the potential energy surface computationally tractable. In other words, SDHTA has 66 normal modes that make it impossible to build up the exact full-dimensional potential energy surface. A careful selection of the degrees of freedom, which reflect the coupling between the hydrogen bonds, is required. This can be done by taking into account those modes which are related to the O-H (D) bond motions (see Fig. 2 for the deuteration scheme), such as the antisymmetric

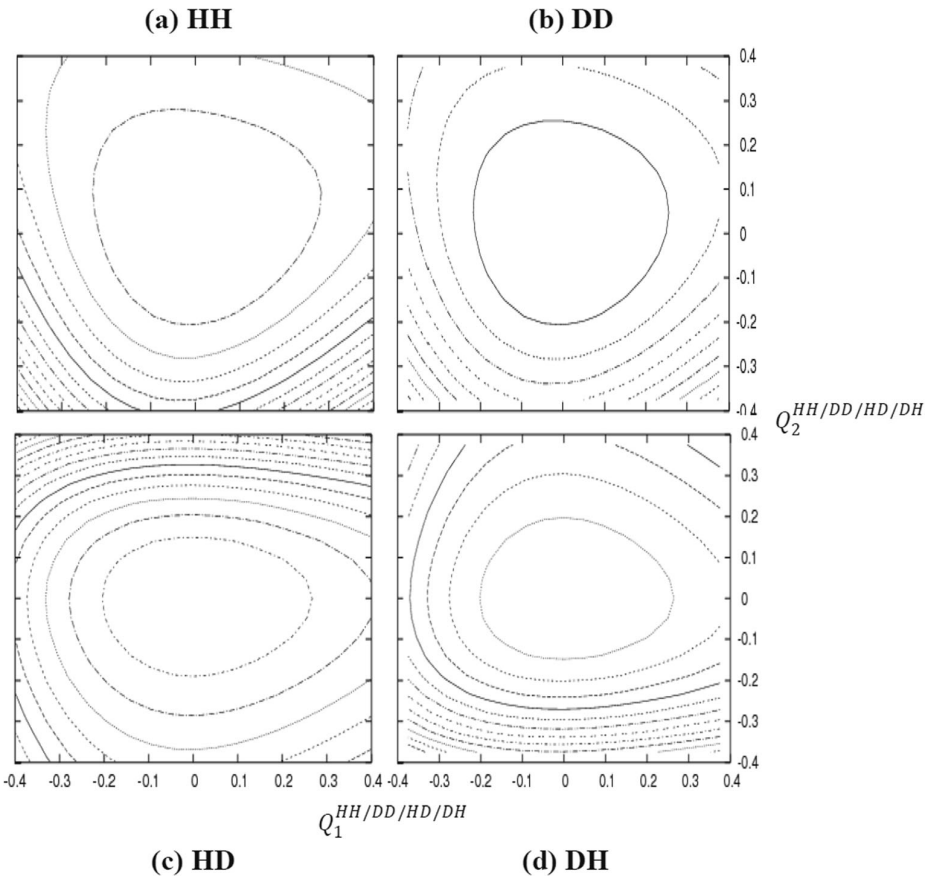

Fig. 5 Two dimensional potential energy surfaces of SDHTA: the contour spacing (in au) is (a) 0.01 to 0.13 in steps of 0.01 (HH case), (b) 0.005 to 0.045 in steps of 0.005 (DD case), (c) 0.005 to 0.07 in steps of 0.005 (HD case), and (d) 0.005 to 0.06 in steps of 0.005 (DHcase)

$Q_1^{HH/DD}$ and symmetric $Q_2^{HH/DD}$ combinations of the O-H stretching vibrations whose normal mode displacements and the corresponding frequencies are shown in Fig. 3. The correlations between the normal modes decrease with increasing the number of the correlated modes. Therefore, it is reasonable to write the potential energy surface up to two-mode correlation terms [26] as:

$$V(Q_1^{HH}, Q_2^{HH}) = V_1^{(1)}(Q_1^{HH}) + V_2^{(1)}(Q_2^{HH}) + V_{12}^{(2)}(Q_1^{HH}, Q_2^{HH}) . \quad (3)$$

Notice that Eq. (3) includes higher order couplings, if any, between each two modes, for instance, $V^2 \sim Q_1^n Q_2^m$. We used 361 points for each two mode potential. Since, the normal mode coordinates are mass-weighted, this procedure is followed for the normal species (HH) and the double H/D isotope symmetric substitution case (DD). The resulting one- and two-dimensional potentials are then fitted to 12th order polynomials using the least-square fitting algorithm. For the asymmetric substitution cases, HD and DH, an explicit two-mode correlation potential has been obtained comprising the two local stretching vibrations Q_1^{HD}, Q_2^{HD}, Q_1^{DH}, and Q_2^{DH}, see Fig. 4. The potential energy surface is analogous to that of Eq. (1).

Figure 5 represents the two dimensional anharmonic potential energy surfaces. They are all asymmetric due to molecular asymmetry and the anharmonic mode-mode coupling. Since the normal modes have been chosen as the employed coordinates, the minima of the potential energy surfaces will remain at $Q = 0$ which correspond to the equilibrium distances in the classical nuclei limit.

Ground-state nuclear wave functions and coupling

The Hamiltonian, Eq. (1), can be implemented in the multiconfiguration time-dependent Hartree approach [27] combined with the imaginary time relaxation technique [28] to calculate the ground state wave functions. The calculations have been performed using the Heidelberg MCTDH program package [29]. For the harmonic oscillators,

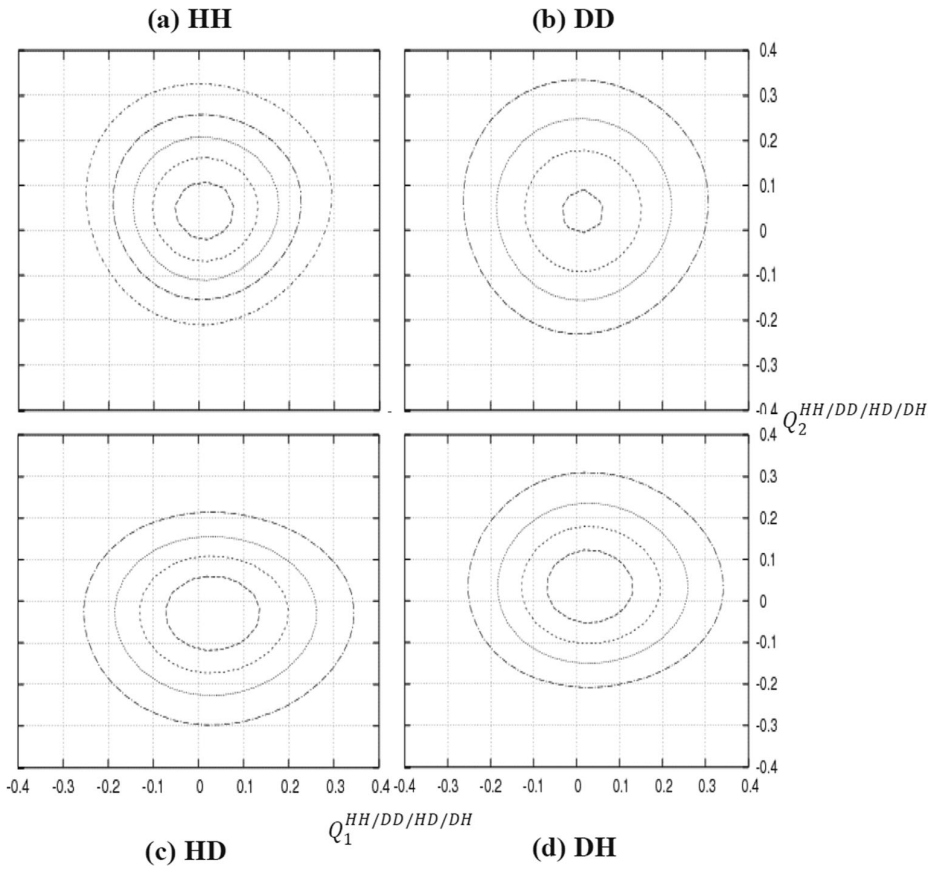

Fig. 6 Two dimensional ground state probability distribution functions of SDHTA: the contour spacing (in au) is (a) 0.05 to 0.25 in steps of 0.05 (HH case), (b) 0.05 to 0.20 in steps of 0.05 (DD case), (c) 0.05 to 0.20 in steps of 0.05 (HD case), (d) 0.05 to 0.20 in steps of 0.05 (DH case)

the discrete variable representation has been used on the grids (in $a_0(amu)^{1/2}$): $Q_{1/2}^{HH/HD/DH/DD}$ [−0.4:0.4] (361 points). Moreover, we used single particle functions describing the combined modes ($Q_1^{HH/DD}Q_2^{HH/DD}$) to capture strong mode-mode couplings. Figure 6 shows the resulting vibrational ground state probability distributions. Inspecting Fig. 5 reveals that the maxima of these distributions do not coincide with the origin due to asymmetry in the potential energy surfaces. For instance, the maximum of the probability density in the case of HH, DH, and DD is shifted to positive $Q_1^{HH/DH/DD}$ and $Q_2^{HH/DH/DD}$, whereas $V^2(Q_1^{HD},Q_2^{HD})$ causes a shift along positive Q_1^{HD} and negative Q_2^{HD}. Quantitatively, the expectation values (in $a_0(amu)^{1/2}$) of the normal modes are calculated to be: $Q_1^{HH}= Q_1^{DD}= 0.02$, $Q_2^{HH}= 0.07$, $Q_2^{DD}= 0.06$, $Q_1^{HD}= 0.04$, $Q_2^{HD}= -0.04$, $Q_1^{DH}= 0.04$, and $Q_2^{DH}= 0.05$.

The calculated expectation values can be used to calculate the corrected geometries by displacing the equilibrium geometry along the normal modes coordi-

Table 2 The hydrogen bond parameters (in Å and degrees) as calculated by the conventional method (classical nuclei) and from the coordinates expectation values for four- and six-dimensional potential energy surfaces of HH/DD and HD, respectively. Some experimental results [21] are given in parenthesis for comparison

	Left hydrogen bond			Right hydrogen bond		
	$R_{O\text{-}H/D}$	$R_{O\ldots H/D}$	$R_{O\text{-}O}$	$R_{O\text{-}H/D}$	$R_{O\ldots H/D}$	$R_{O\text{-}O}$
Classical	1.008	1.606	2.612	1.009	1.598	2.605
HH	1.033	1.582	2.614	1.035 (1.059)	1.574 (1.487)	2.606 (2.546)
DD	1.025	1.591	2.614	1.027	1.583	2.607
DH	1.025	1.591	2.614	1.036 (1.063)	1.573 (1.477)	2.606 (2.540)
HD	1.032	1.587	2.613	1.026	1.583	2.607

Table 3 The normal modes coupled to the displaced mode $Q_1^{HH} = 5a_0(amu)^{1/2}$, their wave numbers, and displacements from the equilibrium position, Q^0

Mode No.	Wavenumber, cm^{-1}	$Q^0\ a_0(amu)^{1/2}$	Mode No.	Wavenumber, cm^{-1}	$Q^0\ a_0(amu)^{1/2}$
1	24	22.77	13	148	2.14
2	34	−49.48	15	199	−6.12
3	38	22.50	16	205	8.09
4	64	3.83	18	273	−1.18
5	63	−2.18	20	463	1.14
6	46	7.96	21	464	−1.22
9	83	8.20	56	2660	1.41
10	102	−1.34	60	3270	1.20
11	107	3.93			

nates according to the calculated expectation values. From the obtained geometries we have calculated the corresponding new hydrogen bond parameters $R_{O\text{-}H}$, $R_{O\text{-}O}$ and $R_{O\ldots H}$ (Table 2) which contain the quantum correction on the anharmonic potential energy surface. Notice that the anharmonicity of the potential energy surfaces combined with the quantum nature of the nuclei causes an O-H bond elongation of about 0.026 Å for the HH case as compared to the classical approximation. As a consequence the hydrogen bond contracts, that is, $R_{O\ldots H}$ shortens by 0.024 Å. Upon double deuteration, the hydrogen bond is weakened. Compared to the HH case the $R_{O\text{-}D}$ distance is shortened by 0.008 Å while $R_{O\ldots H}$ increases by 0.009 Å. Thus, we found the order $R_{OH}^{class} < R_{OH}^{quant}(DD) < R_{OH}^{quant}(HH)$ and $R_{O\ldots H}^{class} > R_{O\ldots H}^{quant}(DD) > R_{O\ldots H}^{quant}(HH)$, i.e., inclusion of the quantum effect leads to a bond that is stronger in the quantum case than the classical one. Moreover, double deuteration causes the quantum effects to diminish, that is, the hydrogen bond becomes weaker.

The change in R_{OO} is not very much observed because the vibrational motion corresponding to the O-O distance is not included in the construction of the potential energy surface. This reflects the multidimensionality of the hydrogen bond and the important coupling between the O-H stretching modes and the O-O vibrational mode. We examined the coupling of all other normal modes to the stretching vibrations by displacing the latter and calculating the forces affecting the other modes in terms of their displacements from the equilibrium position $\left(Q^o\right)$. Tables 3 and 4 represent the normal modes coupled strongly to the stretching vibrations Q_1^{HH} and Q_2^{HH}, respectively. Note that Q^o values lower than 1 $a_0(amu)^{1/2}$ are ignored. Figures 7 and 8 display the displacement vectors of the modes that are coupled strongly to Q_1^{HH} and Q_2^{HH}, respectively (the other modes corresponding to the HD, DH, and DD species are included in the Supporting information). It is obvious that all these modes do not include pure O-O stretching vibrations (neither symmetric nor asymmetric), although there are many oxygen atoms motions. The overall motion of the strongly coupled vibrations may reflect O-O motion, however one cannot implement all these vibrations into the potential energy surface.

Table 4 The normal modes coupled to the displaced mode, $Q_2^{HH} = 5a_0(amu)^{1/2}$, their wave numbers, and displacements from the equilibrium position, Q^0

Mode No.	Wavenumber, cm^{-1}	$Q^0\ a_0(amu)^{1/2}$	Mode No.	Wavenumber, cm^{-1}	$Q^0\ a_0(amu)^{1/2}$
1	50	3.04	10	110	2.63
2	35	29.16	11	114	4.79
3	48	15.05	13	151	−1.03
4	114	−2.86	15	199	−7.28
6	118	2.01	16	204	−4.10
7	76	−4.84	18	272	1.08
8	94	4.14	20	469	1.02
9	92	−4.73	60	2464	1.59

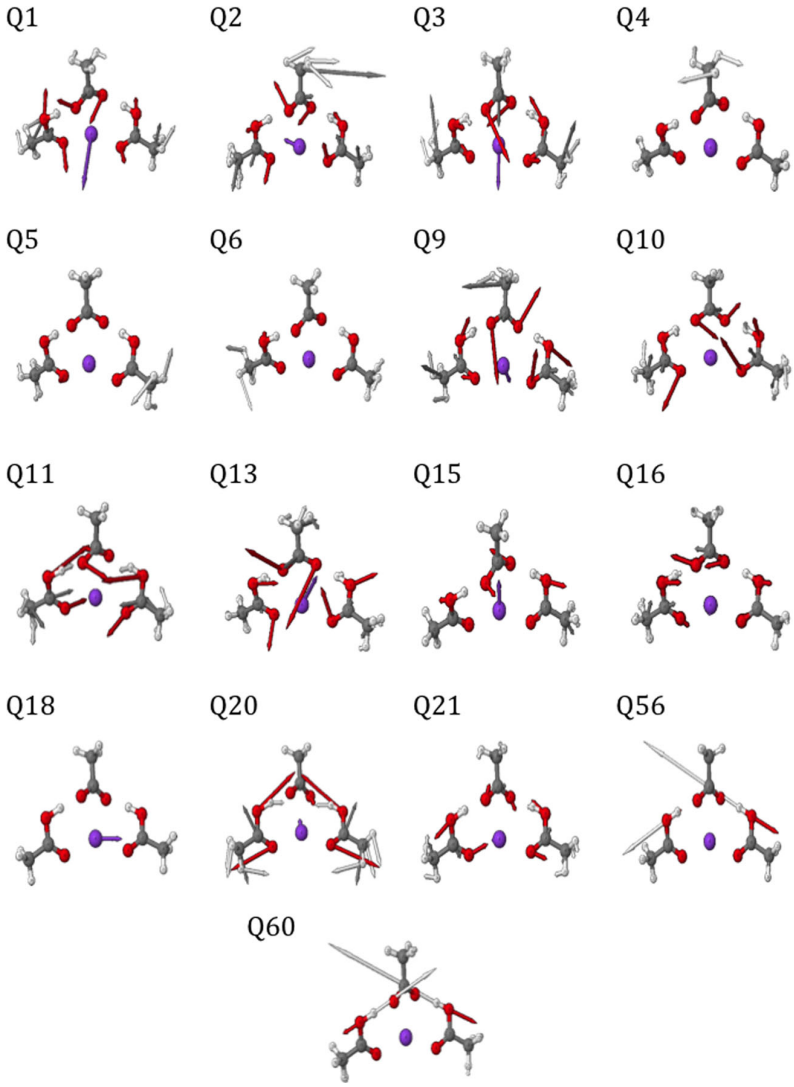

Fig. 7 The mode displacement vectors corresponding to the strongly coupled modes to Q_1^{HH}

Therefore, further study [30] is needed to abstract all these strongly coupled modes into one or two modes, using the method of localized vibrational modes [31, 32], which will then be implemented in the potential energy surface. The resulting three or four-dimensional potential energy surfaces are expected to reflect the effect of the O-O motion on hydrogen bonds coupling [30].

Focusing on the single deuteration case (HD/DH), we observe that the distances R_{OH} and $R_{O...H}$ change upon including quantum effects. In the case of the deuterated bond, the distance R_{OH} is smaller than that of the HH quantum case. On the other hand, $R_{O...H}$ is larger, in the case of deuterated hydrogen bond, than that of the HH quantum case. The changes in R_{OH} and $R_{O...H}$ distances of the deuterated hydrogen bonds do not appear in the non-deuterated bonds. In other words, single substitution leads to a weakening only in the deuterated hydrogen bond as compared to the HH quantum case. These preceding effects reveal that SDHTA comprises uncoupled hydrogen bonds.

Conclusions

In this work the 2D potential anharmonic potential energy surfaces are calculated in terms of normal modes

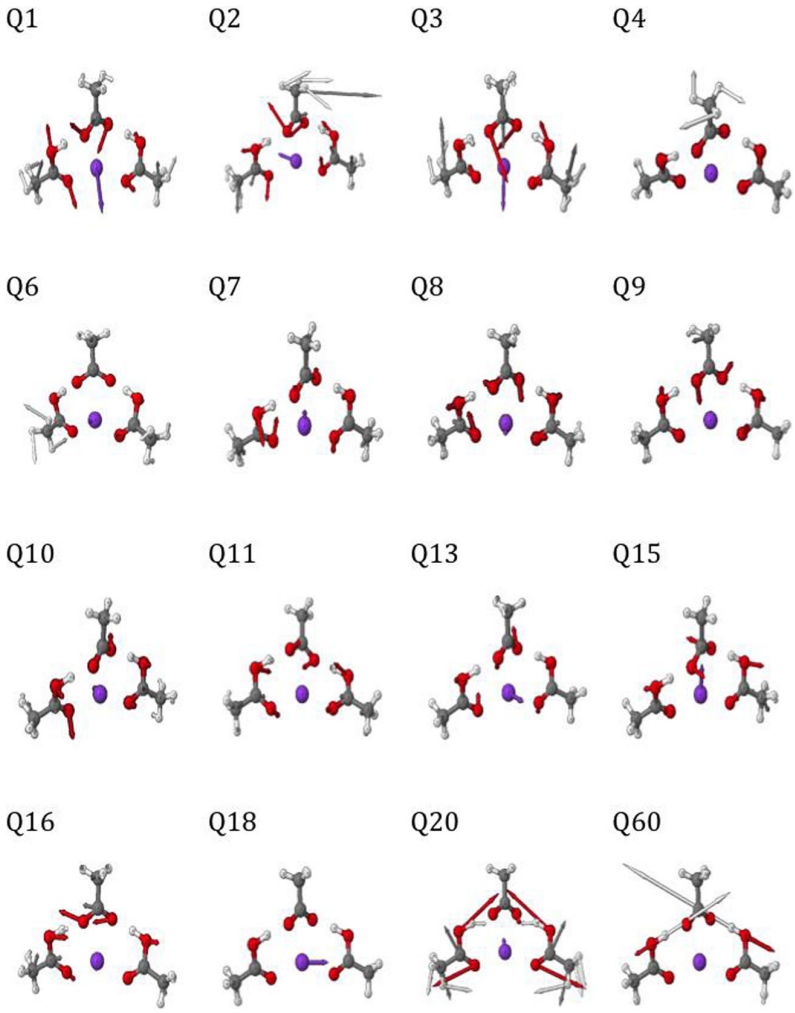

Fig. 8 The mode displacement vectors corresponding to the strongly coupled modes to Q_2^{HH}

that reveal the hydrogen bond motions. Based on the 2D potential energy surfaces combined with the corresponding nuclear wave functions, the double hydrogen bonds in SDHTA are uncoupled. This procedure can be applied for large hydrogen-bonded biological systems, like DNA base pairs, carbohydrate-protein receptor interaction … etc., as normal modes (coordinates) can be easily calculated yet the wave character of hydrogen (quantum particle) and the anharmonic coupling are included. However, the O-O vibrational mode is important to be implemented in the potential energy surfaces to reveal the change of the O-O distance upon deuteration. Further study is needed to implement that much of coupled modes (Fig. 7 and Fig. 8) to the potential energy surfaces based on the methods described in references [31] and [32].

Acknowledgments The authors would like to thank Prof. Dr. Oliver Kühn for his support.

References

1. Lopez de la Paz M, Ellis G, Perez M, Perkins J, JimenezBarbero J, Vicent C (2002) Carbohydrate hydrogen-bonding cooperativity-intramolecular hydrogen bonds and their cooperative effect on intermolecular processes−binding to a hydrogen-bond acceptor molecule. Eur J Org Chem 2002:840–855
2. Gutberlet T, Heinemann U, Steiner M (2001) Protein crystallography with neutrons - status and perspectives. Acta Cryst D57:349–354
3. Novak A (1974) Structure and bonding. -Springer, Berlin-Heidelberg 18:177–216
4. Smirnov SN, Golubev NS, Denisov GS, Benedict H, Schah-Mohammedi P, Limbach H-H (1996) Hydrogen/deuterium isotope effects on the NMR chemical shifts and geometries of intermolecular

low-barrier hydrogen-bonded complexes. J Am Chem Soc 118: 4094–4101
5. Benedict H, Hoelger C, Aguilar-Parrilla F, Fehlhammer WP, Wehlan M, Janoschek R, Limbach H-H (1996) Hydrogen/deuterium isotope effects on the ^{15}N NMR chemical shifts and geometries of low-barrier hydrogen bonds in the solid state. J Mol Struct 378:11–16
6. Lorente P, Shenderovich IG, Golubev NS, Denisov GS, Buntkowsky G, Limbach H-H (2001) $^{1}H/^{15}N$ NMR chemical shielding, dipolar $^{15}N,^{2}H$ coupling and hydrogen bond geometry correlations in a novel series of hydrogen-bonded acid–base complexes of collidine with carboxylic acids. Magn Reson Chem 39:S18–S29
7. Kohen A, Limbach H-H (2005) (eds.) Isotope effects in the biological and chemical sciences, Taylor and Francis, Boca Raton.
8. Li Q, An X, Gong B, Cheng J (2007) Cooperativity between OH···O and CH···O hydrogen bonds involving dimethyl sulfoxide−H_2O−H_2O complex. J Phys Chem A 111:10166–10169
9. Shibl MF, Pietrzak M, Limbach H-H, Kühn O (2007) Geometric H/D isotope effects and cooperativity of the hydrogen bonds in porphycene. Chem Phys Chem 8:315–321
10. Shibl MF, Tachikawa M, Kühn O (2005) The geometric (H/D) isotope effect in porphycene: grid-based Born–Oppenheimer vibrational wavefunctions vs. multi-component molecular orbital theory. Phys Chem Phys 7:1368–1373
11. Jeffrey GA, Saenger W (1991) Hydrogen bonding in biological structures. Springer, New York
12. Schuster P, Zundel G, Sandorfy C (1976) The hydrogen bond. North-Holland, New York
13. Steiner T, Saenger W (1994) Lengthening of the covalent O-H bond in O-H…O hydrogen bonds re-examined from low-temperature neutron diffraction data of organic compounds. Acta Cryst B50: 348–357
14. Gilli P, Bertolasi V, Ferretti V, Gilli G (1994) Covalent nature of the strong homonuclear hydrogen bond. Study of the O-H–O system by crystal structure correlation methods. J Am Chem Soc 116:909–915
15. Jeffrey GA (1997) An introduction to hydrogen bonding. New York, Oxford
16. Nahringbauer I (1969) The crystal structure of the 1:1 addition compound of ammonium acetate and acetic acid. Acta Chem Scand 23:1653–1666
17. Speakman JC, Mills HH (1961) The crystal structures of the acid salts of some monobasic acids. Part VI. Sodium hydrogen diacetate. J Chem Soc 1164–1175
18. Currie M (1972) Crystal structure of potassium tri-hydrogen di-malonate: a neutron diffraction study. J Chem Soc, Chem Commun 972b-973
19. Saito M, Kasai T, Nagai K (1963) The rapid acetylation of rayon (III) retardation of acetylation rate by acetic acid (IV) pretreatment and acetic acid swelling. Sen'I Gakkaishi 19:7–20
20. Ahmed AA, Kühn O, Hilal RH, Shibl MF (2013) Structure and cooperativity of the hydrogen bonds in sodium dihydrogen triacetate. Int J Quant Chem 113:1394–1400
21. Tolstoy PM, Schah-Mohammedi P, Smirnov SN, Golubev NS, Denisov GS, Limbach H-H (2004) Characterization of fluxional hydrogen-bonded complexes of acetic acid and acetate by NMR: geometries and isotope and solvent effects. J Am Chem Soc 126: 5621–5634
22. Becke AD (1993) Density–functional thermochemistry. III. The role of exact exchange. J Chem Phys 98:5648
23. Krishnan R, Seeger JS, Pople JA (1980) Self–consistent molecular orbital methods. XX. A basis set for correlated wave functions. J Chem Phys 72:650
24. Frisch MJ, Trucks GW, Schlegel HB, Scuseria GE, Robb MA, Cheeseman JR, Montgomery Jr J A, Vreven T, Kudin KN, Burant JC, Millam JM, Iyengar SS, Tomasi J, Barone V, Mennucci B, Cossi M, Scalmani G, Rega N, Petersson GA, Nakatsuji H, Hada M, Ehara M, Toyota K, Fukuda R, Hasegawa J, Ishida M, Nakajima T, Honda Y, Kitao O, Nakai H, Klene M, Li X, Knox JE, Hratchian HP, Cross JB, Bakken V, Adamo C, Jaramillo J, Gomperts R, Stratmann RE, Yazyev O, Austin AJ, Cammi R, Pomelli C, Ochterski JW, Ayala PY, Morokuma K, Voth GA, Salvador P, Dannenberg JJ, Zakrzewski VG, Dapprich S, Daniels AD, Strain MC, Farkas O, Malick DK, Rabuck AD, Raghavachari K, Foresman JB, Ortiz JV, Cui Q, Baboul AG, Clifford S, Cioslowski J, Stefanov BB, Liu G, Liashenko A, Piskorz P, Komaromi I, Martin RL, Fox DJ, Keith T, Al-Laham MA, Peng CY, Nanayakkara A, Challacombe M, Gill PMW, Johnson B, Chen W, Wong MW, Gonzalez C, Pople JA (2004) GAUSSIAN 03 (Revision C.02), Gaussian Inc., Wallingford, CT
25. Watson JKG (1968) Simplification of the molecular vibration-rotation hamiltonian. Mol Phys 15:479–490
26. Carter S, Culik SJ, Bowman JM (1997) Vibrational self-consistent field method for many-mode systems: a new approach and application to the vibrations of CO adsorbed on Cu (100). J Chem Phys 107:10458
27. Meyer H-D, Worth GA (2003) Quantum molecular dynamics: propagating wavepackets and density operators using the multiconfiguration time-dependent Hartree method. Theor Chem Acc 109:251–267
28. Kosloff R, Tal-Ezer H (1986) A direct relaxation method for calculating eigenfunctions and eigenvalues of the Schrödinger equation on a grid. Chem Phys Lett 127:223–230
29. Worth GA, Beck MH, Jäckle A, Meyer H-D (2005) The MCTDH package. Version 8.3, University of Heidelberg
30. Ahmed AA, Shibl MF (2014) unpublished
31. Jacob CR, Reiher M (2009) Localizing normal modes in large molecules. J Chem Phys 130:84106
32. Jacob CR, Luber S, Reiher M (2009) Analysis of secondary structure effects on the IR and Raman spectra of polypeptides in terms of localized vibrations. J Phys Chem B 113:6558–6573